Reactive Molecular Dynamics Studies of DMMP Adsorption and Reactivity on Amorphous Silica Surfaces

ARTICLE *in* THE JOURNAL OF PHYSICAL CHEMISTRY C · OCTOBER 2010

Impact Factor: 4.77 · DOI: 10.1021/jp104547u

2 AUTHORS:

Jason Quenneville
Spectral Sciences Incorporated
33 PUBLICATIONS **1,148** CITATIONS
SEE PROFILE

Ramona Taylor
Spectral Sciences Incorporated
21 PUBLICATIONS **532** CITATIONS
SEE PROFILE

Reactive Molecular Dynamics Studies of DMMP Adsorption and Reactivity on Amorphous Silica Surfaces

Jason Quenneville* and Ramona S. Taylor*

Spectral Sciences, Inc., Burlington, Massachusetts 01803, United States

Adri C. T. van Duin

Department of Mechanical and Nuclear Engineering, Pennsylvania State University University Park, Pennsylvania 16802, United States

Received: May 18, 2010; Revised Manuscript Received: September 23, 2010

By using molecular dynamics (MD) computer simulations in conjunction with the ReaxFF reactive force fields, the interaction of dimethyl methylphosphonate (DMMP) with amorphous silica as a function of surface hydration was examined. Surface hydroxylation densities of 2.0, 3.0, 4.0, and 4.5 hydroxyl/nm^2 were modeled. The amorphous silica surface used in our simulations is quantified structurally and compares well to experimental findings. At the higher OH densities, binding of DMMP to the hydroxylated silica was found to occur through a combination of van der Waals interactions and hydrogen bonding. In addition to these types of interactions, at the lower OH surface coverages, strong covalent bonding between the phosphonyl (P═O) oxygen of DMMP and 3-coordinate Si defects on the surface was observed. Finally, at extremely low hydroxyl coverages (2.0 nm^{-2}), DMMP fragmentation was found to occur. The binding energy of DMMP on amorphous silica with a hydroxyl density of 4.5 OH/nm^2 was calculated to be −4.7 kcal/mol. Addition of a water layer to the silica-supported DMMP system showed that water can displace and/or hydrolyze the adsorbed DMMP molecules. To validate the ReaxFF/MD findings, we performed MP2 and DFT quantum chemical studies of reactions predicted by the MD/ReaxFF by using small silica clusters. The quantum chemistry results support the MD/ReaxFF results, providing further verification of our findings and indicating the viability of ReaxFF/MD to study complex surface chemistry.

I. Introduction

Since their introduction in World War I, modern chemical warfare agents (CA) have been utilized in military conflicts such as the Iran-Iraq War and the Soviet invasion of Afghanistan to incapacitate and kill opposing military forces. Today, however, terrorist extremists have extended the threat of a chemical weapons attack to the civilian population. One of the more common types of chemical agent is the nerve agent. Nerve agents, such as sarin and VX, inhibit the body's ability to utilize acetylcholinesterase, which leads to an unhealthy accumulation of acetycholine at the neuro−neuro and neuro−muscular junctions and, eventually, death.[1] The fate of the chemical agent subsequent to its release is important to the safety of the personnel in the immediate vicinity of the release. In addition, the types of interactions that occur between the agent and the environmental elements in its path will determine when, or if, the affected areas can be reclaimed for use. To better understand the fate of CA species, a basic understanding of what influences the reactivity of these species on environmentally relevant materials is required.[2−5]

Experiments have been conducted to understand how CAs and their simulants interact with various environmental target materials, such as sands, soils, and clays.[6−10] In addition, amorphous silicon dioxide (a-SiO_2), a principal component of each of these materials, has been utilized in highly controlled laboratory experiments as a surrogate for these environmental target materials.[11−15] Given the highly toxic nature of the CAs, many of these experiments use a simulant molecule, such as dimethyl methylphosphonate (DMMP), instead of the live CA. DMMP is a common simulant for the organophosphate nerve agents, sarin and VX. Structures for DMMP and sarin are shown Figure 1.

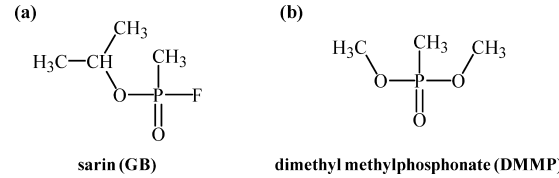

Figure 1. Structures of (a) sarin and (b) dimethyl methylphosphonate (DMMP).

In one of the earliest studies of the interaction of DMMP with a-SiO_2, Henderson and co-workers adsorbed DMMP onto a nonhydrated a-SiO_2 surface at 170 K and monitored its reactivity by using temperature program desorption.[11] The DMMP was completely desorbed from the surface between 200 and 275 K, giving an activation energy for desorption of 16.9 kcal/mol. No decomposition of the DMMP was seen in these experiments. On the other hand, DMMP was found to undergo a small amount of decomposition if the surface was hydrated prior to the DMMP adsorption. In a subsequent study, Kanan and Tripp found via infrared (IR) spectroscopy that DMMP hydrogen bonds to the hydrated a-SiO_2 surface through first its methoxy groups and then its phosphonyl (P═O) group.[12,13] This finding differs from results of DMMP adsorbed on other

* Corresponding authors. E-mail: jasonq@spectral.com and rtaylor@spectral.com.

10.1021/jp104547u
Published on Web 10/19/2010

hydrated metal oxides, such as TiO_2, Al_2O_3, and WO_3, where the strongest interaction was found to be between the surface and the P═O group. In addition, IR studies of the interaction of DMMP with polymeric siloxane materials suggest that the strongest interaction is between the P═O group and the siloxane hydroxyls.[16]

Kanan and Tripp estimated their isolated surface hydroxyl density to be 1.0 SiOH/nm^2.[13] In the open atmosphere, the surface hydroxyl density has been measured to be between 4.6 and 4.9 SiOH/nm^2,[17−19] and under high vacuum conditions, it is approximately 2.6 OH/nm^2.[19,20] Given that the experiments were conducted with such low hydroxyl coverage, questions remain as to how a highly hydroxylated surface will affect the adsorption and subsequent reactivity of DMMP.

With advances in computer technology and computational algorithms, computational chemistry now allows scientists to delve deeper than ever into the molecular and submolecular properties of many complicated chemical systems. Here, we examine the interaction of DMMP with amorphous silica as a function of the surface hydration via molecular dynamics (MD) computer simulations. In addition, the ability of liquid water to displace a DMMP molecule preadsorbed on the SiO_2 surface is also examined. The potential model employed in these calculations is the fully reactive ReaxFF empirical potential which was developed by van Duin and Goddard.[21−24]

ReaxFF is an empirical force field that relates the degree of chemical bonding between two atoms (the bond order) to the distance between them.[25−28] This allows for the efficient treatment of bond formation and breakage (i.e., chemical reactions) in large condensed phase systems. ReaxFF is parametrized against ab initio predictions (typically of equilibrium geometries, reaction energies, and some bulk properties) on a training set that now includes more than 5000 chemical species. The ReaxFF potential energy function is:

$$E_{\text{system}} = (E_{\text{bond}} + E_{\text{over}} + E_{\text{under}}) + E_{\text{angle}} + E_{\text{torsion}} + E_{\text{lone-pair}} + E_{\text{conjugation}} + E_{\text{hydrogen-bonding}} + E_{\text{van-der-Waals}} + E_{\text{Coulomb}}$$

where the individual energy terms represent the bond order term (with *N*-body terms to correct for the possibility of over- or under-coordination of atoms), the bond angle and torsion energies, terms corresponding to the formation/destruction of nonbonding electron pairs and conjugation hydrogen bonding, and van der Waals and Coulombic interactions. In addition, chemical reactions and large geometrical variations can change the charge distribution in the system dramatically; thus, ReaxFF necessarily contains a means for equilibration of atomic charges throughout the course of the simulation.[29]

MD investigations of the structure of liquid DMMP[30] and calculations of reaction cross sections for the interaction of DMMP and sarin with O(^{3}P)[31] have been reported in the literature. In addition, quantum mechanical calculations have been performed to understand the unimolecular decomposition[32] and hydrolysis[33,34] of gas-phase chemical agents and to determine the adsorption energies and structures of a various CA adsorbed on solid surfaces.[35−41] Bermudez utilized density functional theory (DFT) to calculate the optimized geometry for the adsorption of DMMP and sarin on small hydrated silica clusters.[42] In these calculations, the most energetically favored bond formation was one in which two hydrogen bonds formed between the P═O group of DMMP and two independent hydroxyl groups on the SiO_2 cluster. To the best of our knowledge, MD simulations of a chemical agent or simulant interacting with silica have not previously been published.

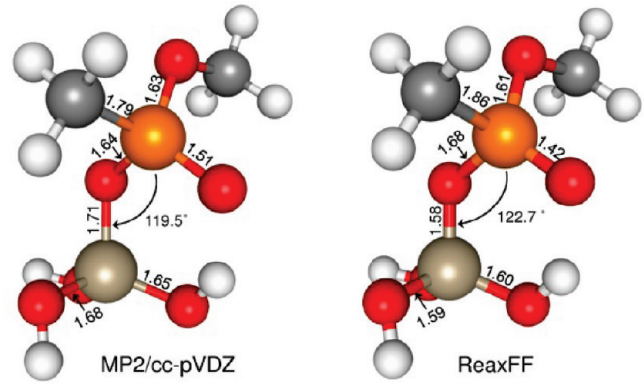

Figure 2. Comparison of the optimized structures of $CH_3OCH_3OP-O-Si(OH)_3$ obtained by using DFT and the ReaxFF reactive force field. $CH_3OCH_3OP-O-Si(OH)_3$ and methanol (CH_3OH) result from the reactive adsorption of DMMP to $Si(OH)_4$. The white, gray, red, orange, and tan spheres represent H, C, O, P, and Si atoms, respectively. Bond lengths are given in angstroms.

The outline of this paper is as follows. The details of the molecular simulations can be found in Sections II and III. The simulation results are discussed in Section III, and the conclusions are given in Section IV.

II. Methodology

The potential energy surface was calculated by using the ReaxFF reactive force field developed by van Duin and Goddard. This potential has been shown to adequately reproduce the energetics and structural properties of the silica and of liquid H_2O.[43]

The ReaxFF parameter set used to describe the interaction of DMMP with the hydroxylated amorphous silica (a-SiO_2) surfaces was constructed for the present study by first combining the parameter sets for bulk silica[44] and phosphoric acid.[45] The parameters for the interaction of silica with phosphoric acid were then optimized by fitting to ab initio data for the reactive adsorption of H_3PO_4 to a $Si(OH)_4$ cluster:

$$H_3PO_4 + Si(OH)_4 \rightarrow (OH)_2OP-O-Si(OH)_3 + H_2O$$

The energy obtained via ReaxFF is 1.2 kcal/mol for this reaction as compared to a reaction energy of 5.1 kcal/mol as calculated via MP2/cc-pVDZ. It should be noted that, in both these reactions, the H_2O molecule formed as a result of the reaction is hydrogen bound to the $(OH)_2OPOSi(OH)_3$ moiety. For the similar reaction of DMMP and $Si(OH)_4$ yielding methanol (CH_3OH) plus the $(OH)_3SiOPOCH_3OCH_3$ compound shown in Figure 2, the geometry and reaction energy of −2.9 kcal/mol obtained with this newly optimized ReaxFF force field are in reasonably good agreement with the ab initio (MP2/cc-pVDZ) results (reaction energy of −6.2 kcal/mol).

All of the MD simulations were run by using the GRASP MD software package developed at Sandia National Laboratories.[46] Unless otherwise stated, all simulations were performed at a temperature of 300 K, and heating was accomplished via a Nose-Hover thermostat with a 2.5 fs time constant. The interatomic cutoff distance for the potential energy and forces was 10 Å, and a time step of 0.25 fs was employed for all simulations.

Quantum chemical calculations were performed both to help parametrize the force field and to validate the important findings of our reactive MD simulations. The MP2 method was used when possible for reaction energies and DFT, with the B3LYP[47] hybrid functional, was used for larger systems and for activation

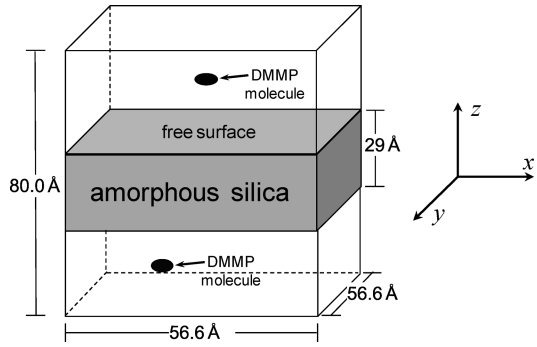

Figure 3. Diagram of the MD simulation cell. Periodic boundary conditions are applied in the x and y directions, and in the z direction, a free surface is allowed to develop at the silica/vacuum interface.

barrier calculations. All calculations were carried out by using the cc-pVDZ[48] basis set and the Gaussian03 quantum chemistry software.[49] No symmetry restrictions were imposed on neither the wave functions nor the geometries.

A. Construction of the Hydroxylated Silica Surfaces. For the simulations described below, a 6191-atom amorphous silica slab was extracted from a previously equilibrated 12 000-atom a-SiO_2 structure to yield a lamella that is 56.6 Å × 56.6 Å × 29 Å.[50−52] The stoichiometric Si/O ratio of this nonhydroxylated silica slab is 1:1.9995. Hydrogen and oxygen atoms are then added to the two exposed surfaces, one in the $-z$ and one in the $+z$ directions, to yield surfaces with the desired hydroxyl densities as discussed below. After hydroxylation, all four silica slabs are charge neutral. As shown in Figure 3, periodic boundary conditions were applied in the x and y directions, with free surfaces in the z directions. By using a Nose-Hover thermostat, this system was equilibrated at 300 K for 10 ps prior to a second 10 ps simulation run in which the temperature was increased linearly from 300 to 1500 K. Lastly, this a-SiO_2 lamella was annealed at 1500 K for 20 ps before a final 10 ps 300 K equilibration period. This equilibration procedure resulted in an equilibrated, but nonhydroxylated, a-SiO_2 lamella with two free surfaces, one in the $+z$ direction and one in the $-z$ direction.

After this initial equilibration process, four distinct silica slab models were prepared with surface hydroxyl densities of 2.0, 3.0, 4.0, and 4.5 hydroxyls/nm^2. The hydroxylation procedure consisted of first adding free hydrogen atoms to the 1-coordinated surface oxygen atoms and hydroxide groups to the 3-coordinate surface silicon atoms and then equilibrating this new system for 500 fs. This process was repeated until the desired surface hydroxyl coverage was obtained. For the higher OH coverages, the temperature of the system was increased from 300 to 3000 K to facilitate this process. After the desired hydroxyl surface density was obtained, a 10 ps temperature ramp was applied to cool the entire system down to 300 K.

Finally, a DMMP molecule was placed approximately 10 Å away from each of the two free SiO_2 surfaces as shown in Figure 3. The x and y coordinates of each DMMP molecule were chosen randomly to give a uniform distribution of impact points on each of the silica surfaces. The initial conditions for each of the DMMP molecules were set such that the temperature of the vibrational and rotational degrees of freedom was approximately 300 K. This was accomplished by equilibrating a box of 250 DMMP molecules at 300 K and randomly selecting one of these molecules for each of the DMMP/surface simulations. The DMMP molecules were then given an initial center-of-mass velocity in either the $-z$ or the $+z$ direction (i.e., pointing toward one of the silica surfaces), corresponding to the most probable velocity, $v_{mp} = (2kT/m)^{1/2}$, for a translational temperature of 300 K. For each of the hydrated a-SiO_2 surfaces discussed above, 50 MD trajectories (each with two DMMP molecules) were performed to give a total of 100 DMMP impingements. Each trajectory was run for 5 ps.

III. Results and Discussion

A. Comparison of a-SiO_2 Surface as a Function of Hydroxyl Coverage. Amorphous silica is composed of SiO_2 tetrahedra that bond via a distorted end-to-end arrangement. When cleaved, the surfaces of these noncrystalline solids are readily hydrated. It is the presence of these surface silanol groups that govern the reactivity of the silica surface. Experiments have identified two types of surface silanol groups: terminal silanols in which a single OH group is attached to an $(-O)_3Si$ group and geminal silanols in which two OH groups are attached to an $(-O)_2Si$ group. If two terminal or geminal silanols are connected by a siloxane bridge, they are deemed vicinal. Terminal and geminal silanols can hydrogen bond with their neighbors to form associated silanol groups, or they may remain isolated and, hence, not be involved in surface hydrogen bonding.

In the open atmosphere, the surface hydroxyl density has been measured to be between 4.6 and 4.9 SiOH/nm^2.[17−19] Whereas, under high vacuum conditions, the hydroxyl density has been found to be approximately 2.6 OH/nm^2.[19,20] Here, we have examined the reactivity of the a-SiO_2 surface to DMMP at four different hydration levels: 2.0 3.0, 4.0, and 4.5 OH/nm^2. Snapshots of the 2.0 and 4.5 OH/nm^2 a-SiO_2 surfaces are shown in Figure 4. In both cases, the silanols are randomly distributed on the surface. Hydrogen bonding between the silanol groups is found at both coverages. In Figure 4, the yellow and green circles highlight examples of terminal and geminal silanol groups. The percentage of geminal surface silanol groups is listed in Table 1. The ReaxFF MD results for the 4.5 OH/nm^2 surface compare well to the experimental value of 10−30%.

In addition, the percentage of vicinal surface silanol groups, the average Si−O and O−H bond distances, and the Si−O−H, O−Si−O, and Si−O−Si bond angles are also given in Table 1. Independent of the hydroxyl area density, the Si−O nearest-neighbor bond length is tightly distributed around 1.57 Å in the bulk region of the silica slab and around 1.58 Å on the surface of the slab. These values are slightly smaller than the experimentally determined Si−O bond length of 1.62 Å.[53] At the lower hydroxyl coverages, the O−H bond length distribution peaks at 0.96 Å, and the distribution peaks at 0.97 Å for the 4.5 OH/nm^2 hydroxy coverage. These values are in good agreement with recent periodic density functional calculations on hydroxylated amorphous silica systems which predict the O−H bond length to be 0.955 Å.[54]

In both the bulk and the surface regions of all four systems, the O−Si−O bond angles are broadly distributed about 108° with the extrema of the distribution being at 90 and 145°, respectively. In the 2.0 and 3.0 OH/nm^2 systems, a small secondary peak at approximately 81° was also seen in the O−Si−O angle distribution calculated for the surface regions. This is in agreement with calculations by Du and Cormack which conclude that this new peak corresponds to small, surface active, Si_xO_y ring species.[52] This peak decreases in size with increasing surface hydroxyl concentration. For all four systems, the Si−O−Si angle distributions peak at 156° for the bulk regions of the amorphous silica slab and at 153−154° for the surface regions which is again in agreement with previous calculations on this system.[52,54]

Finally, the Si−O−H bond angle for the silanol species was found to peak between 111 and 112°. Unlike the O−Si−O and

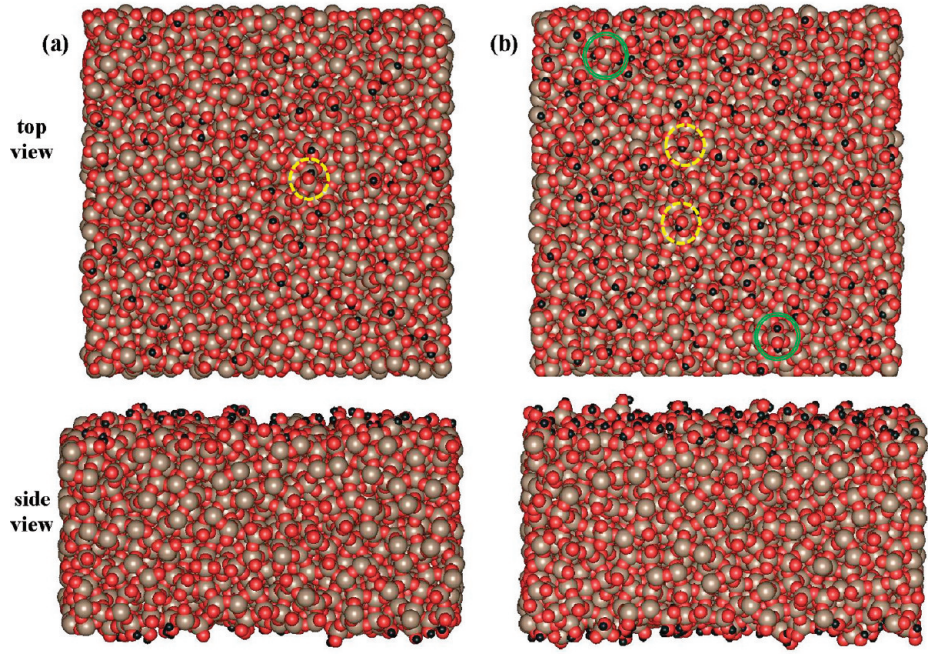

Figure 4. Top and side views of the (a) 2.0 hydroxyl/nm^2 and (b) 4.5 hydroxyl/nm^2 a-SiO_2 surfaces. The yellow and green circles highlight examples of terminal and geminal silanol groups, respectively. The tan, red, and dark gray spheres represent Si, O, and H atoms, respectively.

TABLE 1: Structural Information for the Four Hydrated Silica Surfaces Used in This Study[a]

property	surface OH density 2.0 nm^{-2}	3.0 nm^{-2}	4.0 nm^{-2}	4.5 nm^{-2}
% geminal silanols	5.3	7.2	14.8	17.0
% vicinal silanols	18.0	29.9	39.3	43.9
r_{Si-O} (Å)	1.57 (1.58)	1.57 (1.58)	1.57 (1.58)	1.57 (1.58)
r_{O-H} (Å, surface)	0.96	0.96	0.96	0.97
Si−O−H angle (deg)	111	111	112	111
O−Si−O angle (deg)	108	108	108	108
Si−O−Si angle (deg)	156 (154)	156 (154)	156 (154)	156 (153)

[a] For the bond lengths and angles, the value at the surface is given in parentheses if it differs from that found in the bulk region of the silica slab.

Si−O−Si bond angles, because no silanol species existed in the bulk regions of the four systems, the Si−O−H bond angle was calculated only for species in the surface regions. The Si−O−H bond angle for hydrated silica surfaces has recently been measured via NMR to be 121°.[55] Hence, the ReaxFF potentials that we are using underestimate this angle; thus, the ReaxFF-obtained surfaces do not have the surface OH groups sticking out from the bulk as much as would be predicted by the NMR experiments. Overall, however, the structures obtained for these hydrated amorphous silica system are in good agreement with previous findings for these systems.

B. Interaction of DMMP with Hydrated a-SiO_2. The reactivity of DMMP was determined for each of the hydrated a-SiO_2 surfaces discussed above. For all four surfaces, all of the impinging DMMP molecules were found to adsorb onto the silica surface via a combination of van der Waals interactions, hydrogen bonding, and covalent bonding. After the impinging DMMP molecule contacts the surface, it diffuses over a small region of the surface and eventually binds to the surface. At 300 K, the kinetic energy of the impinging DMMP molecule is large enough to allow the molecule to diffuse about the surface before sticking. Thus, much more of the a-SiO_2 surface is sampled than would be indicated by the 100 aiming points utilized in the trajectories.

The results of the MD simulations are summarized in Table 2 which gives the percentage of DMMP molecules that adsorb through van der Waals forces, hydrogen bonding, and covalent bonding. It should be noted that each adsorption event was classified according to its strongest interaction. For example, if a trajectory resulted in DMMP having both a covalent bond and a hydrogen bond, this event was classified as having resulted in a covalent bond. DMMP is considered to be adsorbed via van der Waals interactions to the a-SiO_2 surface if the distance between the DMMP molecule and any of the surface atoms is less than the sum of the van der Waals radii of the two interacting atoms plus a preset cutoff distance:

$$d_{ij} < r_i + r_j + d_{\text{cutoff}} \quad (1)$$

TABLE 2: Types of Adsorption Observed for DMMP Impinging upon an Amorphous silica Surface As a Function of the Surface Hydroxyl Density[a]

adsorption type	surface OH density 2.0 nm^{-2}	3.0 nm^{-2}	4.0 nm^{-2}	4.5 nm^{-2}
van der Waals	49	57	59	63
hydrogen bonding	19	34	38	37
covalent	32	9	3	0

[a] For each coverage, 100 DMMP impingement events were followed. All trajectories resulted in at least part of the DMMP molecule adsorbing to the surface.

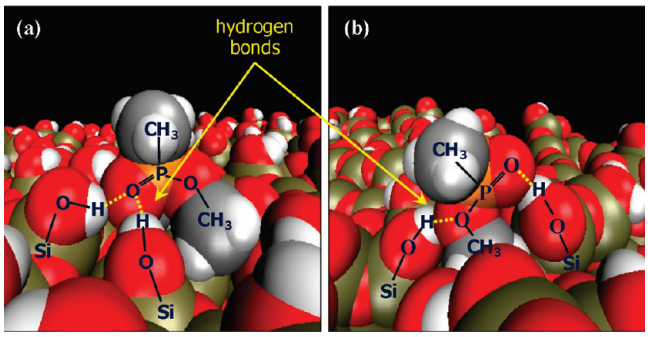

Figure 5. Snapshots of two hydrogen bonding trajectories taken after 5.0 ps of simulation time. In (a), hydrogen bonds are formed between the phosphonyl oxygen on the DMMP molecule and two surfaces silanol groups. In (b), hydrogen bonds are formed between surface silanols and both the methoxy oxygen and the phosphonyl oxygen of DMMP. For both snapshots, the surface hydroxyl density is 4.5 OH/nm^2. The color scheme is the same as that used in Figure 2.

where d_{ij} is the distance between a given surface atom and the closest atom in the DMMP molecule, r_i and r_j are the van der Waals radii of these two atoms, and d_{cutoff} is 0.1 Å. Hydrogen atoms are not explicitly counted in this analysis; instead, the effective van der Waals radius of the atom to which they are bound (either C or O) is adjusted appropriately. Covalent bonds are determined in a similar manner except that the van der Waals radii in eq 1 are replaced by the covalent radii of the atoms and the cutoff distance, d_{cutoff}, is increased to 0.5 Å. Hydrogen-bonding interactions are said to occur if the O···H distance is less than 2.5 Å and the O···H−O angle is greater than or equal to 135°.

At the end of the 5 ps simulation time, van der Waals interactions between the impinging DMMP molecule and the surface were found to be present in all of the trajectories. However, as described above, the DMMP adsorption is only classified as being of the van der Waals type if covalent or hydrogen bonding interactions do not exist. Consequently, the percentage of van der Waals bound DMMP reflects the fraction of DMMP that is only weakly bound to the surface. Some of the van der Waals classified adsorption events involve a DMMP molecule that is still mobile. Given that each trajectory is stopped after 5 ps, it is possible that these weakly bound molecules might eventually desorb from the surface at some later time. The ultimate fate of these molecules is left for future work, but we anticipate that stronger adsorption via hydrogen or covalent bonding will occur for much of this fraction.

For the three highest OH coverages, the second most common type of interaction after van der Waals between the impinging DMMP molecule and the a-SiO_2 surface was via hydrogen bonding. As expected, adsorption due to hydrogen bonding increases as the surface hydroxyl area density increases from 2.0 to 3.0 nm^{-2} but somewhat surprisingly remains steady at hydroxyl coverages above 3.0 nm^{-2}.

At all four hydroxyl coverages, the two most common hydrogen-bonding arrangements found in these simulations involve a hydrogen bond forming either between the phosphonyl oxygen of DMMP and a surface silanol group or between one of DMMP's two methoxy oxygen groups and a surface silanol. At the high hydroxyl coverages, multiple hydrogen bonds often formed between the DMMP and more than one surface silanol group. Two examples of these are shown in Figure 5. In Figure 5a, two separate hydrogen bonds are formed between the phosphonyl oxygen on DMMP and two distinct terminal silanol groups on the surface. In contrast, in Figure 5b, the hydrogen

TABLE 3: Percentage of Defect Sites As a Function of Surface Hydroxyl Density

	surface OH density			
defect type	2.0 nm^{-2}	3.0 nm^{-2}	4.0 nm^{-2}	4.5 nm^{-2}
% 1-coordinate O atoms	0.67	0.19	0.02	0.07
% 3-coordinate O atoms	0.81	0.55	0.31	0.30
% 3-coordinate Si atoms	2.37	1.65	1.11	1.16

bonds formed between DMMP and the surface involve both the phosphonyl oxygen and one of the methoxy oxygens on DMMP. Experiments by Kanan and Tripp[12,13] using IR spectroscopy have suggested that the main type of hydrogen-bonding arrangement involves a surface silanol group and a methoxy oxygen on DMMP. Bermudez examined this configuration and found instead that the energetically most favorable hydrogen bonding configuration was between the phosphonyl oxygen group of DMMP and either one or two surface silanol groups.[42] For the 3.0, 4.0, and 4.5 OH/nm^2 coverages, 77% of the observed hydrogen bonds were between a surface silanol group and the phosphonyl oxygen of DMMP as compared to only 19% between a silanol and DMMP's methoxy oxygen. In the remaining 4% of the observed hydrogen-bonding events, hydrogen bonds formed between the a-SiO_2 surface and both the phosphonyl and the methoxy oxygens of DMMP as shown in Figure 5b. Finally, in 8% of the hydrogen-bonding events involving only the phosphonyl oxygen of DMMP, two surface-DMMP hydrogen bonds were formed as shown in Figure 5a.

At the 2.0 OH/nm^2 coverage, however, this is not the case. Here, only 53% of the observed hydrogen bonds involved the phosphonyl group of DMMP, 41% occurred between the methoxy oxygen of DMMP and the surface, and the remaining 6% included hydrogen bonds that were formed between the surface and both the phosphonyl and the methoxy oxygens. Kanan and Tripp estimated the OH coverage on the silica surfaces used in their experiments to be 1.0 OH/nm^2.[13] In contrast, experiments by Zhuravlev[56] suggest that Kanan's and Tripp's silica surfaces would instead have a hydroxyl coverage of 2.3 OH/nm^2. Although different, both experiments indicate that the experimental findings of Kanan and Tripp are best compared to our simulations at 2.0 OH/nm^2 coverage. At this OH surface density, our simulations show that the fraction of DMMP molecules that hydrogen bond through the methoxy oxygen increases, in agreement with the results of Kanan and Tripp. We attribute this increase to a shift toward a less hydrophilic surface, which should help accommodate the methyl portion of the methoxy moiety that approaches closely to the surface in this hydrogen-bond configuration.

In agreement with experiments, at a hydroxyl density of 4.5 OH/nm^2, DMMP does not covalently bind to this hydrated silica surface. However, at lower hydroxyl coverages, the number of reactive defect sites increases. The three predominant types of defect sites on a-SiO_2 include the overcoordinated 3-coordinate oxygen atom, the under-coordinated 1-coordinate oxygen and 3-coordinate silicon atoms. As shown in Table 3, the percentage of each of these types of defect sites increases with decreasing surface hydration. Interestingly, DMMP adsorption via covalent bonding also increases with decreasing surface OH density. An examination of the trajectories which result in the formation of covalently bound DMMP shows that the creation of a covalent DMMP/a-SiO_2 bond always involves a surface defect site. The most common type of chemical reaction predicted by our MD/ReaxFF studies of the interaction of DMMP with the hydrated a-SiO_2 surface involves the covalent attachment of DMMP to the silica surface through the formation of a Si−O bond between

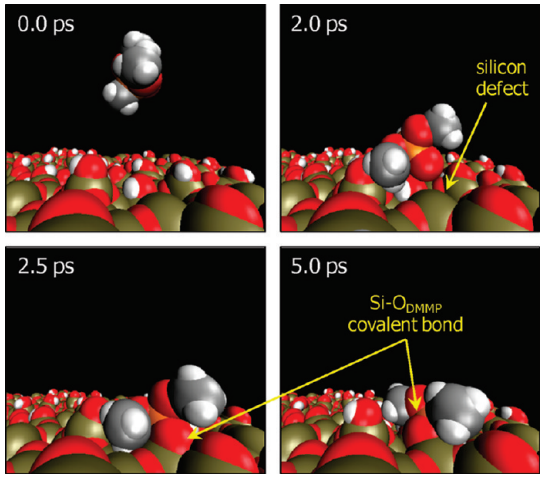

Figure 6. Time slices from a trajectory in which DMMP covalently bonds to the a-SiO_2 surface. At 0 ps, the center-of-mass velocity of the impinging DMMP molecule is normal to the silica surface. After 2.5 ps, the DMMP molecule is covalently bonded to the surface through a Si−O bond that formed between the phosphonyl oxygen of DMMP and a 3-coordinate Si defect on the surface. In this simulation, the surface hydroxyl density is 3.0 nm^{-2}. The color scheme is the same as that described in the caption for Figure 2.

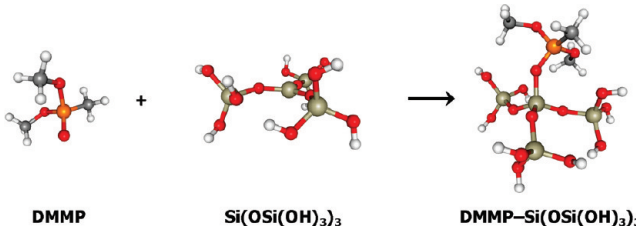

Figure 7. Geometry-optimized structures for the reaction of DMMP with a $Si[OSi(OH)_3]_3$ cluster to yield the covalently adsorbed DMMP/$Si[OSi(OH)_3]_3$ reaction product. The reaction energy calculated with ReaxFF (−85.6 kcal/mol) for this reaction compares well with that determined via a MP2/cc-pVDZ calculation (−87.0 kcal/mol). The color scheme is the same as that used in Figure 2.

the double-bonded O atom of the DMMP and a dangling (3-coordinate) Si atom defect on the surface (Figure 6).

The reaction of DMMP with a 3-coordinate Si atom to yield a covalently bonded DMMP/SiO_2 entity was not included in the reaction training set for ReaxFF force-field parameter optimization. Hence, to verify that our ReaxFF parametrization accurately describes the energetics of this reaction, the reaction energy for the interaction of DMMP with a $Si[OSi(OH)_4]_3$ cluster determined by the ReaxFF potential was compared to that determined via an MP2/cc-pVDZ calculation for this same reaction (Figure 7). Given the computational expense of the MP2 method, the 3-coordinate surface Si site was modeled by a $Si[OSi(OH)_3]_3$ cluster in these calculations. The MP2/cc-pVDZ reaction energy of −87.0 kcal/mol agrees well with the −85.6 kcal/mol reaction energy predicted by the ReaxFF potential. This is an example of a reaction channel which was first identified via ReaxFF and then validated via ab initio calculations.

Fragmentation of the DMMP molecule, although rare, was observed on the 2.0, 3.0, and 4.0 OH/nm^2 surfaces. No fragmentation of DMMP molecule was observed at the highest hydroxyl coverage, 4.5 OH/nm^2. On the 2.0 OH/nm^2 hydroxylated a-SiO_2 surface, the impinging DMMP molecules underwent some degree of fragmentation in 17% of the trajectories. This number decreased to 6 and 1% on the 3.0 and 4.0 OH/nm^2 a-SiO_2 surfaces, respectively. In all cases, fragmentation of the DMMP molecule resulted in the covalent bonding of a CH_3 group to the a-SiO_2 surface. Hence, these reactions are counted as covalent reactions in Table 2. All of the observed fragmentation events involved the abstraction of the methoxy methyl group from DMMP as shown in Figure 8. In the trajectory shown here, the impinging DMMP molecule interacts with an under-coordinated oxygen atom on the a-SiO_2 surface. The result of this interaction is the abstraction of a CH_3 group from DMMP to form a surface methoxy group. The remaining $O_2P(CH_3)OCH_3$ entity binds to the surface through van-der-Waals-type interactions. If this trajectory were to be continued for longer than the initial 5 ps simulation period, it is expected that this $O_2P(CH_3)OCH_3$ species would further react with the surface.

The methylation reaction of a $OSi(OSi(OH)_3)_3$ cluster through homolytic cleavage of one of the O−CH_3 bonds in DMMP and methylation of the 1-coordinate oxygen atom on the silica cluster is shown in Figure 9. This reaction was studied with DFT by using a radical mechanism (i.e., because the calculations are performed in vacuum, all species have zero charge) and was found to have a reaction energy of −10 kcal/mol. In contrast, the ReaxFF force field predicts a reaction energy of −43 kcal/mol. Unfortunately, our model silica cluster is quite small. Consequently, it is not clear that it can faithfully represent the larger silica surface used in the MD simulations. If this cluster is representative of the larger silica nanoparticle, our current ReaxFF force field overestimates the reactivity of these 1-coordinate oxygen defect sites by ∼30 kcal/mol. However, even given this increased reactivity, at surface hydroxyl densities representative of atmospheric conditions, these reactions remain rare events and only become a significant proportion of the observed DMMP/a-SiO_2 interactions at severely low hydroxyl

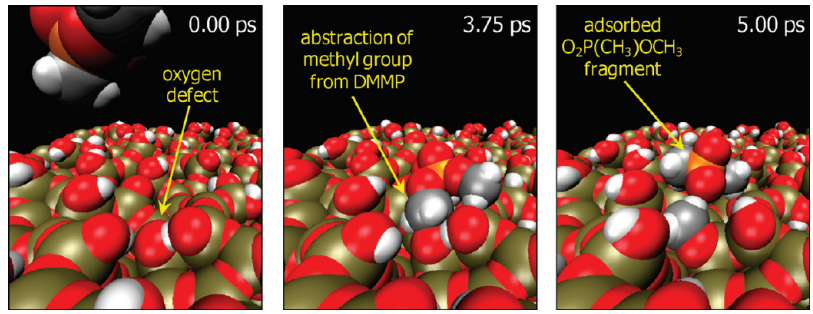

Figure 8. Time slices along a MD trajectory which results in the fragmentation of the impinging DMMP molecule. At the beginning of the trajectory, a 1-coordinate oxygen defect is present on the surface. At 0 ps, this under-coordinated oxygen is hydrogen-bound to two other surface silanol groups. At 3.75 ps, this under-coordinated oxygen abstracts a methyl group from one DMMP methoxy groups. As seen at 5.0 ps, this abstraction process results in an adsorbed surface methoxy group and a weekly adsorbed $O_2P(CH_3)OCH_3$ species. In this simulation, the area density of hydroxyl groups on the silica surface is 4.0 nm^{-2}, and the color scheme is the same as that described in the caption for Figure 2.

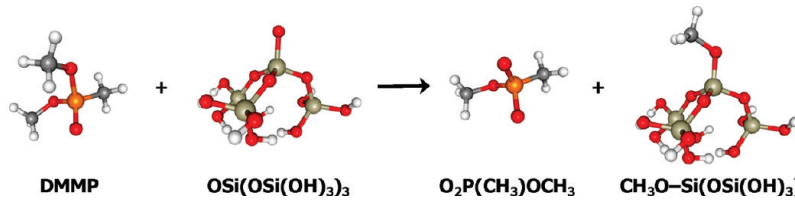

Figure 9. Geometry-optimized structures for the reaction of DMMP with a $SiO[OSi(OH)_3]_3$ radical cluster. This reaction results in the homolytic cleavage of one of the $O-CH_3$ bonds in DMMP and the methylation of the 1-coordinate O atom in the cluster. The corresponding reaction energies determined by the ReaxFF potential and a series of BLY3P/cc-pVDZ DFT calculations are −43.0 and −10.0 kcal/mol, respectively.

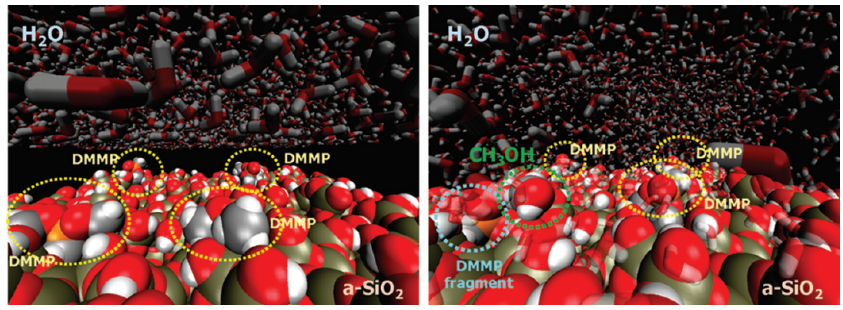

Figure 10. Snapshots from a MD simulation in which water has been introduced onto a hydrated a-SiO_2 surface with preadsorbed DMMP molecules. The left panel is the initial configuration with four DMMP molecules adsorbed onto one of the two surfaces, and water is initially suspended ~3 Å above a hydrated a-SiO_2 surface which had four DMMP molecules preadsorbed to it (left panel). The right panel shows this same system at a later time ($t = 81.35$ ps). Three of the four DMMP molecules remain adsorbed to the surface. The fourth, however, has undergone reaction to form a solvated methanol species and an adsorbed DMMP fragment. (Note: this simulation was periodic in all dimensions; thus, although only one surface of the lamella is shown, the top of the water layer was is in contact with the bottom of the a-SiO_2 lamella which had another four DMMP molecules preadsorbed to it.)

densities. This discrepancy between the DFT and the ReaxFF-predicted reactivity of these oxygen defect sites will be a topic for further study.

C. Calculation of DMMP/hydrated a-SiO_2 Adsorption Energy. To quantify the average adsorption energy of DMMP on silica, we performed an MD simulation with eight DMMP molecules adsorbed onto the 4.5 OH/nm^2 hydrated a-SiO_2 lamella. Four DMMP molecules were adsorbed to each of the two free surfaces of the silica slab by using the same procedure as that described in Section II. Approximately 50 Å of vacuum separates the two surfaces. The total potential energy of the system was averaged over 50 ps and compared to the sum of the average potential energies for the a-SiO_2 slab and DMMP molecules alone. In this way, the adsorption energy of DMMP on hydrated a-SiO_2 was calculated to be −4.7 kcal/mol. On average, 37.5% of the DMMP molecules (three of the eight molecules) are hydrogen-bonded to the surface during the course of the simulation. None of the molecules are covalently bound. As shown in Table 2, at 4.5 nm^{-2} hydroxyl coverage, 37 out of 100 trajectories resulted in DMMP hydrogen-bound to the surface. Thus, our simulation containing only eight adsorbate molecules is a remarkably faithful representation of a much larger ensemble of trajectories, and our calculated adsorption energy of −4.7 kcal/mol should be considered as the average adsorption energy for DMMP adsorbed on a-SiO_2 at near-atmospheric surface hydration densities.

D. Fate of Adsorbed DMMP on a-SiO_2 in the Presence of H_2O. An important question in the subject of agent adsorption onto environmental substrates is whether, once adsorbed onto the substrate, the agent can be displaced from the substrate by water during a rain event. To investigate the effect of a surface water layer, a MD simulation was run in which bulk H_2O was added to the DMMP/hydrated a-SiO_2 simulation cell following the adsorption of eight DMMP molecules on the silica slab as described in Section III.C. After 20 ps of equilibration, bulk water was inserted into the vacuum region between the two free surfaces. The inserted water lamella contained 4000 H_2O molecules which had previously been equilibrated under constant density conditions (1.0 g/cm^3) for 20 ps at 300 K. As shown in Figure 10, directly after insertion, a 3 Å gap existed between the bulk-like H_2O lamella and the closest atom on each of the two DMMP/a-SiO_2 surfaces. Subsequent to the insertion of the bulk water layer, an 80 ps constant volume trajectory was performed for this new H_2O/DMMP/a-SiO_2 system to examine the fate of the adsorbed DMMP molecules in the presence of liquid H_2O.

As described above, at the beginning of the simulation, three of the eight DMMP molecules are hydrogen-bonded to the a-SiO_2 surface, and the remaining five DMMP molecules are adsorbed via van der Waals interactions. During the course of the 80 ps of equilibration, however, one of the adsorbed H_2O molecules is removed from the surface. As shown in the right panel of Figure 10, 62 ps after the bulk water layer is added to the system, only seven of the eight DMMP molecules remain adsorbed to the a-SiO_2 substrate. Interestingly, one of the DMMP molecules has undergone acid-catalyzed hydrolysis to yield a solvated CH_3OH moiety and an adsorbed DMMP fragment.

The feasibility of this reaction was validated with quantum chemistry. In vacuum, the reaction energy for the formation of methanol through reaction of a water molecule with DMMP is calculated to be −0.9 and +0.6 kcal/mol with ReaxFF and MP2, respectively. By using the self-consistent reaction-field method and the polarized continuum model (as implemented in Gaussian03),[49] we estimate that the MP2 reaction energy decreases to −2.4 kcal/mol in aqueous solution. In addition, DFT predicts the activation energy barrier for this hydrolysis reaction to be 47.8 kcal/mol in vacuum but only 2.1 kcal/mol in aqueous solution. Therefore, quantum chemistry results not only verify that the MD/ReaxFF prediction of DMMP hydrolysis is correct but also suggest that it should be a fairly common decomposition reaction in humid conditions.

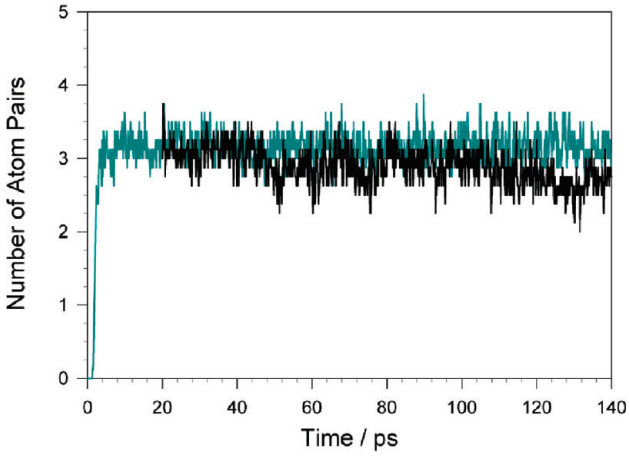

Figure 11. Average number of DMMP/silica atom pairs with attractive van der Waals interactions as a function of time. The cyan lines were calculated for a DMMP/hydrated a-SiO_2 system where no H_2O was present, and the black lines were calculated for a similar system in the presence of water. Here, the water was added to the simulation cell 20 ps after the DMMP molecules were adsorbed to the hydrated a-SiO_2 surface.

The bonding between the DMMP and the a-SiO_2 surface is shown as a function of time in Figure 11. As shown by the cyan line, in the absence of H_2O, the number of pairwise van der Waals interactions between each DMMP molecule and the surface remains relatively constant over the 140 ps time span of the simulation. In contrast, the addition of water weakens the dispersive binding of the DMMP to the surface (black line in Figure 11). This effect is slight on the time scale of our simulation but could become more pronounced at later times as more of the DMMP molecules either react with or are displaced by the water.

To the best of our knowledge, these simulations are the first to show that DMMP molecules adsorbed on silica surfaces not only can be displaced by H_2O but also can undergo reaction with the water to yield more benign reaction products. Future work is planned to better understand how the structure of the silica surface affects the absorption strength of the DMMP/silica complex. In addition, similar types of simulations are planned to examine the interaction of DMMP on other surfaces such as TiO_2 and Al_2O_3.

IV. Conclusion

MD simulations using the reactive ReaxFF potential were performed to examine the interaction of DMMP with hydrated amorphous silica surfaces both in the presence and in the absence of water. The nature of the adsorption of DMMP on silica was found to depend strongly on the hydroxyl coverage of the silica surface. At sufficiently high coverage, ~37% of the DMMP molecules hydrogen-bond to the surface. As the surface hydration decreases, the surface defect density increases, and the reactivity of DMMP increases along with it. Although rare, when DMMP does react with the silica surface, DMMP can covalently attach to the surface and, less frequently, fragment to yield adsorbed methyl species. At the highest hydroxyl coverage studied (4.5 nm^{-2} area density), the average adsorption energy of DMMP on silica at near-atmospheric hydration coverages was determined to be −4.7 kcal/mol.

Our reactive MD simulations with the ReaxFF force field identified a number of chemical reactions important in the interaction of DMMP with hydrated amorphous silica. These reactions were investigated with quantum chemical methods for verification. In general, good agreement was found between the ReaxFF and quantum chemical predictions. Investigation of the associated activation barriers as well as refinement of the force-field parameters for these reactions are left for future studies.

In nature, bulk quantities of water will typically be present when chemical agents come in contact with environmental substrates such as a-SiO_2. Given that chemistry is often facilitated in solution relative to vacuum, the presence of bulk water could dramatically affect the fate of the agent by facilitating chemical reactions not captured with a simple surface/vacuum-interface model. To examine this effect, MD simulations were performed to examine the fate of DMMP molecules which had been preadsorbed on the silica surface to the addition of bulk quantities of water. These simulations, although in their early stages, predict that adsorbed DMMP can react with water to yield solvated methanol species. We plan to investigate this reaction in more depth during future studies.

Ultimately, one would like to understand not only the reactivity and fate of the chemical simulants in the contact with silica and water but also the fate of live chemical agents. Work is currently underway to expand the ReaxFF to include the halogen/phosphate/silica parameter sets needed to investigate sarin and/or VX with hydrated silica.

Acknowledgment. The authors would like to thank Drs. Stephen Lee and Jennifer Becker at the Army Research Office for their support of this work. In addition, the authors would like to thank Professor Rene Corrales at the University of Arizona for graciously providing us with coordinates for our initial amorphous silica system and Dr. Aidan P. Thompson at Sandia National Laboratories for allowing us to use the GRASP molecular dynamics program. This work is supported through the HDTRA CBDIF program under contract number HDTRA 1-07-C-0098.

References and Notes

(1) Hurley, M. M.; Wright, J. B.; Lushington, G. H.; White, W. E. *Theor. Chem. Acc.* **2003**, *109*, 160.
(2) Bizzigotti, G. O.; Castelly, H.; Hafez, A. M.; Smith, W. H. B.; Whitmire, M. T. *Chem. Rev.* **2009**, *109*, 236.
(3) Wesely, M. L. *Atmos. Environ.* **1989**, *23*, 1293.
(4) Mackay, D.; Guardo, A. D.; Kicsi, G.; Cowan, C. E. *Environ. Toxicol. Chem.* **1996**, *15*, 1618.
(5) Bartelt-Hunt, S.; Barlaz, M. A.; Knappe, D. R. U.; Kjeldsen, P. *Environ. Sci. Technol.* **2006**, *40*, 4219.
(6) Montauban, C.; Begos, A.; Bellier, B. *Anal. Chem.* **2004**, *76*, 2791.
(7) Brevett, C. A. S.; Sumpter, K. B.; Pence, J.; Nickol, R. G.; King, B. E.; Giannaras, C. V.; Durst, H. D. *J. Phys. Chem. C* **2009**, *113*, 6622.
(8) Wagner, G. W.; O'Connor, R. J.; Procell, L. R. *Langmuir* **2001**, *17*, 4336.
(9) D'Agostino, P. A.; Hancock, J. R.; Provost, L. R. *J. Chromatography A* **2001**, *912*, 291.
(10) Groenewold, G. S.; Williams, J. M.; Appelhans, A. D.; Gresham, G. L.; Olson, J. E.; Jeffery, M. T.; Rowland, B. *Environ. Sci. Tehcnol.* **2002**, *36*, 4790.
(11) Henderson, M. A.; Jin, T.; White, J. M. *J. Phys. Chem.* **1986**, *90*, 4607.
(12) Kanan, S. M.; Tripp, C. P. *Langmuir* **2001**, *17*, 2213.
(13) Kanan, S. M.; Tripp, C. P. *Langmuir* **2002**, *18*, 722.
(14) Gay, I. D.; McFarlan, A. J.; Morrow, B. A. *J. Phys. Chem.* **1991**, *95*, 1360.
(15) Ekerdt, J. G.; Klabunde, K. J.; Shapley, J. R.; White, J. M.; Yates, J. T., Jr. *J. Phys. Chem.* **1988**, *92*, 6182.
(16) Ferguson-McPherson, M. K.; Low, E. R.; Esker, A. R.; Morris, J. R. *Langmuir* **2005**, *21*, 11226.
(17) Kinney, D. R.; Chuang, I. S.; Maciel, G. E. *J. Am. Chem. Soc.* **1993**, *115*, 8695.
(18) Lange, K. R. *J. Colloid Sci.* **1965**, *20*, 231.
(19) D'Souza, A. S.; Pantano, C. G. *J. Am. Ceram. Soc.* **1999**, *82*, 1289.
(20) Du, J.; Cormack, A. N. *J. Am. Ceram. Soc.* **2005**, *88*, 2532.
(21) van Duin, A. C. T.; Dasgupta, S.; Lorant, F., III. *J. Phys. Chem. A* **2001**, *105*, 9396.

(22) Van Duin, A. C. T.; Strachan, A.; Stewman, S.; Zhang, Q.; Xu, X., III. *J. Phys. Chem. A* **2003**, *107*, 3803.
(23) Chenoweth, K.; Cheung, S.; van Duin, A. C. T.; Goddard, W. A., III.; Kober, E. M. *J. Am. Chem. Soc.* **2005**, *127*, 7192.
(24) Strachan, A.; Kober, E. M.; van Duin, A. C. T.; Oxgaard, J., III. *J. Chem. Phys.* **2005**, *122*, 054502.
(25) Abell, G. C. *Phys. Rev. B* **1985**, *31*, 6184.
(26) Tersoff, J. *Phys. Rev. Lett.* **1986**, *56*, 632. Tersoff, J. *Phys. Rev. B* **1989**, *39*, 5566.
(27) Brenner, D. W. *Phys. Rev. B* **1990**, *42*, 9458.
(28) Brenner, D. W.; Shenderova, O. A.; Harrison, J. A.; Stuart, S. J.; Ni, B.; Sinnott, S. B. *J. Phys.: Condens. Matter* **2002**, *14*, 783.
(29) Mortier, W. J.; Ghosh, S. K.; Shankar, S. J. *J. Am. Chem. Soc.* **1986**, *108*, 4315.
(30) Vishnyakov, A.; Neimark, A. V. *J. Phys. Chem. A* **2004**, *108*, 1435.
(31) Conforti, P. F.; Braunstein, M.; Dodd, J. A. *J. Phys. Chem. A* **2009**, *113*, 13752.
(32) Yang, L.; Shroll, R. M.; Zhang, J.; Lourdaraj, U.; Hase, W. L. *J. Phys. Chem. A.* **2009**, *113*, 13762.
(33) Seckute, J.; Menke, J. L.; Emnett, R. J.; Patterson, E. V.; Cramer, C. J. *J. Org. Chem.* **2005**, *70*, 8649.
(34) Daniel, K. A.; Kopff, L. A.; Patterson, E. V. *J. Phys. Org. Chem.* **2008**, *21*, 321.
(35) Michalkova, A.; Gorb, L.; Ilchenko, M.; Zhikol, O. A.; Shishkin, O. V.; Leszczynski, J. *J. Phys. Chem. B* **2004**, *108*, 1918.
(36) Michalkova, A.; Ilchenko, M.; Gorb, L.; Leszczynski, J. *J. Phys. Chem. B* **2004**, *108*, 5294.
(37) Gorb, L.; Lutchyn, R.; Zub, Y.; Leszczynski, D.; Leszczynski, J. *J. Molec. Struct.* **2006**, *766*, 151.
(38) Michalkova, A.; Martinez, J.; Zhikol, O. A.; Gorb, L.; Shishkin, O. V.; Leszczynski, D.; Leszczynski, J. *J. Phys. Chem. B* **2006**, *110*, 21175.
(39) Bermudez, V. M. *Surf. Sci.* **2008**, *602*, 1938.
(40) Bermudez, V. M. *J. Phys. Chem. C* **2009**, *113*, 1917.
(41) Taylor, R. S.; Guiang, C.; Shroll, R. M. *Determining the Reactivity of Chemical Warfare Agents on Metal Oxide Surfaces via Computational Chemistry*, Proceedings of Chemical and Biological Defense Physical Science and Technology Conference; November 17−21 2008, New Orleans.
(42) Bermudez, V. M. *J. Phys. Chem. C* **2007**, *111*, 9314.
(43) Raymand, D.; van Duin, A. C. T.; Spångberg, D.; Goddard, W. A., III.; Hermannson K. Surf. Sci., **2010**, accepted for publication.
(44) van Duin, A. C. T.; Strachan, A.; Stewman, S.; Zhang, Q., III. *J. Phys. Chem. A* **2003**, *107*, 3803.
(45) Zhu, R.; Janetzko, F.; Zhang, Y.; van Duin, A. C. T.; Goddard, W. A., III.; Salahub, D. R. *Theor. Chem. Acc.* **2008**, *120*, 479.
(46) Thompson, A. P. *GRASP: General Reactive Atomistic Simulation Program*, v4.0; Sandia National Laboratories, 2005.
(47) Stephens, P. J.; Devlin, F. J.; Chabalowski, C. F.; Frisch, M. J. *J. Phys. Chem.* **1994**, *98*, 11623.
(48) Dunning, T. H. *J. Chem. Phys.* **1989**, *90*, 1007.
(49) Frisch, M. J.; Trucks, G. W.; Schlegel, H. B.; Scuseria, G. E.; Robb, M. A.; Cheeseman, J. R.; Montgomery, Jr., J. A.; Vreven, T.; Kudin, K. N.; Burant, J. C.; Millam, J. M.; Iyengar, S. S.; Tomasi, J.; Barone, V.; Mennucci, B.; Cossi, M.; Scalmani, G.; Rega, N.; Petersson, G. A.; Nakatsuji, H.; Hada, M.; Ehara, M.; Toyota, K.; Fukuda, R.; Hasegawa, J.; Ishida, M.; Nakajima, T.; Honda, Y.; Kitao, O.; Nakai, H.; Klene, M.; Li, X.; Knox, J. E.; Hratchian, H. P.; Cross, J. B.; Bakken, V.; Adamo, C.; Jaramillo, J.; Gomperts, R.; Stratmann, R. E.; Yazyev, O.; Austin, A. J.; Cammi, R.; Pomelli, C.; Ochterski, J. W.; Ayala, P. Y.; Morokuma, K.; Voth, G. A.; Salvador, P.; Dannenberg, J. J.; Zakrzewski, V. G.; Dapprich, S.; Daniels, A. D.; Strain, M. C.; Farkas, O.; Malick, D. K., Rabuck, A. D.; Raghavachari, K.; Foresman, J. B.; Ortiz, J. V.; Cui, Q.; Baboul, A. G.; Clifford, S.; Cioslowski, J.; Stefanov, B. B.; Liu, G.; Liashenko, A.; Piskorz, P.; Komaromi, I.; Martin, R. L.; Fox, D. J.; Keith, T.; Al-Laham, M. A.; Peng, C. Y.; Nanayakkara, A.; Challacombe, M.; Gill, P. M. W.; Johnson, B.; Chen, W.; Wong, M. W.; Gonzalez, C. Pople, J. A., *Gaussian 03*, Revision C.02 Gaussian, Inc.: Wallingford, CT, 2004.
(50) The initial 12 000-atom amorphous silica crystal was graciously provided by Professor René Corrales of the University of Arizona. It was equilibrated by using the SiO_2 potential of Du and Cormack.[51,52] More details about the initial equilibration process can be found in ref 51.
(51) Du, J.; Corrales, L. R. *Nucl. Instrum. Methods Phys. Res., Sect. B* **2007**, *255*, 177.
(52) Du, J.; Cormack, A. N. *J. Non-Cryst. Solids* **2005**, *351*, 2263.
(53) Mozzi, R. L.; Warren, B. E. *J. Appl. Crystallogr.* **1969**, *2*, 164.
(54) Tielens, R.; Gervais, C.; Lambert, J. F.; Mauri, F.; Costa, D. *Chem. Mater.* **2008**, *20*, 3336.
(55) Kobayashi, T.; DiVerdi, J. A.; Maciel, G. E. *J. Phys. Chem. C.* **2008**, *112*, 4315.
(56) Zhuravlev, L. T. *Langmuir* **1987**, *3*, 316.

JP104547U